Enabling AUV Mapping of Free-Drifting Icebergs Without External Navigation Aids

Marcus Hammond* and Stephen M. Rock*†
*Stanford University, †MBARI

***Abstract*—This paper documents improvements in the method for offline estimation of iceberg geometry as presented by Kimball and Rock [1]. The method removes the AUV's inertial position from the equations, allowing the mission to be completed without ship-based navigation aids. This is a substantial operational advantage. Additionally, it differs from [1] in that it treats each sonar return individually, instead of abstracting multiple readings to a single point, removing a potential source of bias. Finally it reformulates the problem to simplify greatly the estimation optimization by reducing the number of needed estimation parameters. Together, these changes yield speed increases of roughly three orders of magnitude, with no loss in accuracy. The method is demonstrated via full simulation of an AUV operating around a free drifting iceberg. Additionally, an underwater sea cliff in Monterey Canyon is used as an iceberg surrogate to test the method on field data.**

I. Introduction

The work presented in this paper aims to enable precision navigation of Autonomous Underwater Vehicles (AUVs) near free-drifting icebergs. Icebergs are of interest to scientists for their roles in climate science and as hosts to complex ecosystems [2]. However, close-up study of icebergs presents a number of hazards to ships and their crew. In order to study them more closely from a safe distance, AUVs and tethered Remotely Operated Vehicles (ROVs) are often used [3].

In [1], Kimball identified Terrain Relative Navigation (TRN) as a good candidate for this mission, but recognized the difficulty in obtaining an accurate map of moving terrain. Underwater mapping typically involves generating a best estimate of a vehicle's path through the environment and then projecting sonar readings out to create a map. However, conventional means of robot localization, such as interferometry, inertial guidance, and GPS are not feasible when the terrain being mapped is moving.

To solve this problem, Kimball developed a technique by which the iceberg's translation and rotation over the duration of the mapping mission could be estimated offline and subtracted during map generation. This work extends his method with improvements in speed, accuracy, and operational limitations.

II. Related Work

A. Navigating Around Ice

Numerous research projects have used AUVs under or around polar ice, and have employed a number of strategies to deal with the navigational challenges peculiar to these conditions. Some of these challenges include reduced effectiveness of inertial sensors at high latitudes and inability to surface to obtain GPS navigation fixes due to ice coverage. One example is MIT Sea Grant's Odyssey II Vehicle. It used integrated inertial measurements to determine attitude and heading, using magnetic intensity measurements to eliminate drift. [4] This was done via post-processing and was not used for real-time navigation. Navigation was performed via LBL sonar beacons deployed through the ice, and a homing beacon was used to navigate back to the extraction point. In another mission, Monterey Bay Aquarium Research Institute's ALTEX AUV was able to get dead-reckoning navigation performance of less than 0.05% distance traveled using a bottom-pinging Doppler Velocity Logger (DVL) and without external navigation aids [5]. Other examples exist, but nearly all of them involve navigating around fast ice (ice fixed to land) or ice floes whose motion is so slow that they can be approximated as stationary over the duration of the mission[6], [7].

One notable exception is the work by Kimball and Rock, [1] who looked at mapping and navigation around free-drifting Antarctic icebergs. These icebergs are driven by ocean currents and winds, and can translate and rotate in heading by large amounts over the course of an AUV traversal. Once the vehicle positions and sonar soundings are projected into the iceberg reference frame, these motions manifest themselves as large errors in dead-reckoned positions and heading; to the vehicle, the iceberg's motion is indistinguishable from unmodeled sensor drift unless some additional information can be found to correct it. To eliminate these apparent drifts, Kimball identified regions of sonar coverage from the beginning and end of a traversal, and used this loop closure to estimate a constant motion profile that would enforce map self-consistency [1]. If the iceberg's motion is not constant throughout the run, the motion model will have errors. Errors in estimated iceberg velocity manifest as warping in the resulting map from the true geometry. Small amounts of map error are tolerable for TRN, but if the vehicle is equipped with DVL, it is then possible to refine the Iceberg motion estimate somewhat. Kimball discusses a method to incorporate this information into the shape estimation to make the estimated trajectory agree more closely with those measurements.

B. Iceberg Motion

Iceberg motion varies with location, size, weather conditions, and currents, but typical figures are 0.03 – 0.08 m/s translation and 5 – 10 deg/s. For typical AUV operating speeds, this motion can translate into an apparent dead-

978-1-4799-4918-2/14/$31.00 ©2014 IEEE

reckoning drift of over 4% of distance traveled [8], as described in the previous section, even while using DVL. This is quite large compared with the typical performance of $\leq 0.1\%$ discussed above.

C. Non-Newtonian Mapping in Other Fields

There has been substantial work in the Structure from Motion community on a variety of methods to reconstruct the shape of objects by making repeated observations while either the object or the observer moves. Some approaches have relied on computer vision, which typically requires some means of establishing correspondence between recognizable image features. [9]

Other methods use a more active approach, such as structured light or LIDAR [10]. These methods can generate dense, three-dimensional point clouds that can be correlated using methods like iterative closest point (ICP) [11] to estimate the relative motion of the observer between observations.

All of these methods share the trait that they do not require information about the inertial motion of the observer or object to perform reconstruction. As such, they provide insight into the problem of mapping a drifting iceberg. However, sensing limitations, described in the following sections, prevent their direct application and necessitate an approach more tailored to the mission's particular characteristics.

III. Approach

The work presented in this paper extends the method devised by Kimball and Rock, described in detail in [1] and [12]. While the overall approach remains unchanged, the extensions yield significant speed increases and operational flexibility.

A. Mathematical Notation

The notation used in this paper includes:

Position vectors are written as

$$\vec{r}^{\,A/B}$$

where A is the "to" point and B is the "from" point.

Unit vectors are denoted with a hat ($\hat{}$), and scalars are unadorned. Note: a hat can also indicate that the quantity is estimated. The meaning should be clear from context, especially when both hat and vector arrow are present.

Velocities are written as

$${}^{A}\vec{v}^{P}$$

which should be read as "the velocity of point P in reference frame A."

Angular velocities are written as

$${}^{A}\vec{\omega}^{B}$$

which should be read as "the angular velocity of reference frame B in reference frame A."

Vector *bases* will be denoted with right subscripts. For example ${}^{I}\vec{v}^{P}_{Q}$ is the velocity of point P through reference frame I, *expressed in* reference frame Q. When taking *derivatives*, left superscripts refer to the reference frame in which the derivative is being taken.

$$\frac{{}^{A}d(\ )}{dt}$$

Points are defined as:

O = Origin, fixed in inertial frame
V_{cm} = Vehicle (Collocated with DVL)
B_{cm} = Iceberg center of mass
S_i = Sounding location (fixed in iceberg frame)

Reference frames are denoted using:

I = Inertial
V = Vehicle
B = Iceberg

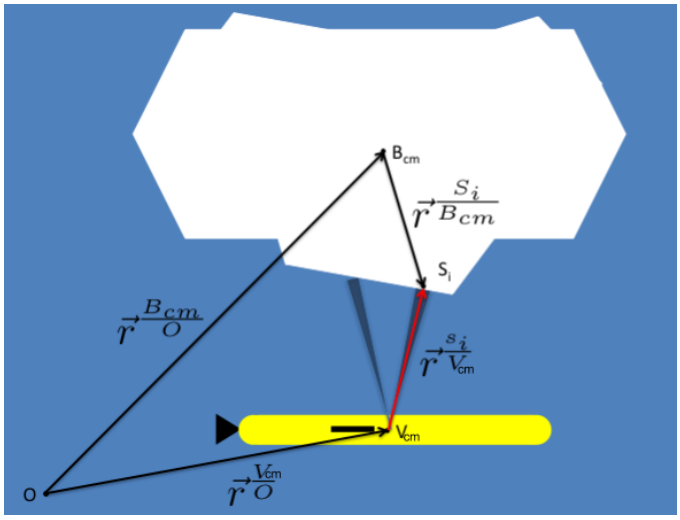

Fig. 1. Vector definitions for iceberg mapping problem

B. Vehicle and Sensor Characteristics

The vehicle model used for this paper is similar to the Dorado-class AUV. This is a torpedo-shaped vessel that achieves control through vectored thrust. As such, the vehicle is turn-radius constrained.

This paper assumes that the AUV being used is equipped with a sideways-facing DVL such that all four beams are nominally incident on the side of the iceberg. With this configuration, the AUV maintains "bottom lock" or "iceberg lock" on the iceberg, giving it a measurement of its velocity in the iceberg's reference frame. The AUV is also assumed to have a multibeam sonar aligned with the scan plane perpendicular to the vehicle's nominal velocity, used for mapping.

It is assumed that the AUV can maintain a constant depth through the use of absolute pressure sensors. This reduces the estimation to a 2D-problem.

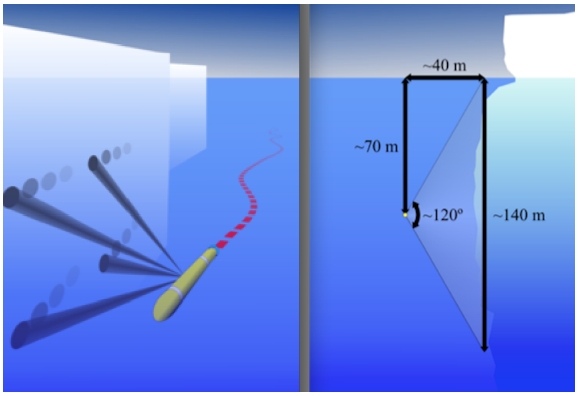

Fig. 2. Orientation of DVL and multibeam beams with respect to AUV. *Graphic courtesy of Peter Kimball*

For each sonar sounding from both the multibeam and DVL, a range is returned. Since the each beam's orientation in the vehicle frame is known, each measurement can be represented as a vector expressed in the vehicle's frame of reference.

The DVL returns velocity information as well. Specifically, it measures the frequency shift of the returned signal, which corresponds directly to the instantaneous rate of change of the length of the DVL beam $\left(\frac{d||\vec{r}^{\,s_i/V_{cm}}||}{dt}\right)$. This is the component of the vehicle's velocity in the iceberg reference frame in the direction of the sonar beam. An important subtlety in this measurement is that the DVL only provides the velocity *as expressed in the vehicle's frame of reference.* It provides no information about vehicle attitude or attitude rates.

$$\underbrace{{}^{I}\vec{v}_{I}^{V_{cm}}}_{\text{Useful for navigation}} = \underbrace{{}^{I}R^{B}}_{\text{Orientation}} \underbrace{{}^{I}\vec{v}_{B}^{V_{cm}}}_{\text{From DVL}} \tag{1}$$

Thus DVL alone cannot provide full velocity information. Normally, an IMU can provide the necessary attitude information, but in the case of navigating relative to a free-drifting iceberg, there is an ambiguity in the vehicle's heading due to the iceberg's freedom to rotate in the horizontal plane. As the following sections will show, determining the vehicle's heading in the iceberg's reference frame is the key: If the heading can be estimated accurately, an accurate and self-consistent map can be constructed.

C. Optimization Setup

1) Overview of Original Method: The method, originally devised by Kimball, is formulated as an iterative nonlinear multi-objective least squares problem in which a quadratic cost function is minimized by estimating iceberg heading and translation over the course of the mapping run. The method uses B-splines as described in [13] to model the iceberg motion. A relatively small number of spline control points can be estimated that generate a smooth estimate of the motion.

For example:

$$\begin{aligned} {}^{I}\hat{\vec{x}}_b(t) &= B_{1,D_x}(t)I\vec{P}_{x,1} + \ldots + B_{N_x,D_x}(t)I\vec{P}_{x,N_x} && (2)\\ &= B_x(t)\vec{P}_x && (3)\\ {}^{I}\hat{\psi}_b(t) &= B_{1,D_\psi}(t)\vec{P}_{\psi,1} + \ldots + B_{N_\psi,D_\psi}(t)\vec{P}_{\psi,N_\psi} && (4)\\ &= B_\psi(t)\vec{P}_\psi && (5) \end{aligned}$$

where the $B(t)$ terms are basis functions and the $\vec{P}$ terms are control points.

Additionally, Kimball introduces a number of "map points" – points fixed on the surface of the iceberg – and estimates their positions.

To perform the optimization, the problem is split into nonlinear and linear parts. The heading spline parameters are chosen in the (nonlinear) outer loop, and are given to the linear inner loop. Given the heading, the best estimate of translation can be estimated explicitly through the method of least squares. The residuals of this process are used to drive the outer loop optimization through a gradient-based nonlinear optimizer. This process is depicted in block diagram form in Figure 3

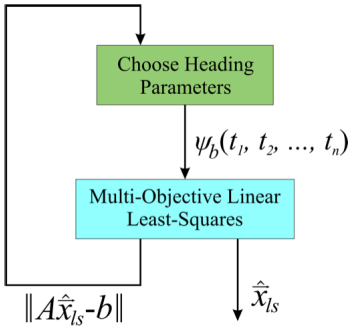

Fig. 3. Inner and outer optimization loops. *Graphic courtesy of Peter Kimball*

Developing the least squares optimization problem defined by matrices A and b involves writing a series of equations which describe loop closure, iceberg heading, position, velocity, etc. Kimball provides details of these equations in [12].

2) Modification to Use Raw Sonar Ranges: The iceberg position, vehicle position and sonar measurements can be related through the vector loop equation, illustrated in Figure 1:

$$\vec{r}^{\,V_{cm}/O} + \vec{r}^{\,S_i/V_{cm}} = \vec{r}^{\,B_{cm}/O} + \vec{r}^{\,S_i/B_{cm}} \tag{6}$$

In Kimball's formulation of the optimization, the points S_i were actually averages of several DVL beams, calculated by fitting a plane to the returns and calculating the centroid. This was done because the method required assigning a full 3-dimensional velocity to each "sounding," but each individual sonar return only carries partial velocity information. By

abstracting the multiple beams into a single approximate point, he was able to assign a velocity to the point. Although the errors introduced by this planar approximation are small, they will always tend to underestimate the radius to the ensonified points from the iceberg's center, and thus introduce a potential source for bias.

Differentiating Eq. 6 yields:

$$\frac{^I d}{dt}(\vec{r}^{\,^{Vcm/O}} + \vec{r}^{\,^{S_i/V_{cm}}} = \vec{r}^{\,^{Bcm/O}} + \vec{r}^{\,^{S_i/B_{cm}}}) \quad (7)$$

$$^I\vec{v}^{V_{cm}} + \frac{^I d}{dt}(\vec{r}^{\,^{S_i/V_{cm}}}) = {}^I\vec{v}^{B_{cm}} + \frac{^I d}{dt}(\vec{r}^{\,^{S_i/B_{cm}}}) \quad (8)$$

$$^I\vec{v}^{V_{cm}} + \frac{^V d}{dt}(\vec{r}^{\,^{S_i/V_{cm}}}) + {}^I\vec{\omega}^{V_{cm}} \times \vec{r}^{\,^{S_i/V_{cm}}} =$$

$$^I\vec{v}^{B_{cm}} + \underbrace{\frac{^B d}{dt}(\vec{r}^{\,^{S_i/B_{cm}}})}_{0} + {}^I\vec{\omega}^B \times \vec{r}^{\,^{S_i/B_{cm}}}. \quad (9)$$

By the definition of S_i as the point ensonified by the DVL, $\vec{r}^{\,^{S_i/V_{cm}}}$ can be rewritten as $r_{i,t}\hat{d}_i$, where $\hat{d}_i$ is the fixed (in vehicle frame) unit vector of the i_{th} DVL beam and $r_{i,t}$ is the corresponding range measurement at time t.

Taking the dot product of this equation with $\hat{d}_i$ yields,

$$\hat{d}_i \cdot {}^I\vec{v}^{V_{cm}} + \dot{r}_{i,t} + \underbrace{\hat{d}_i \cdot {}^I\vec{\omega}^{V_{cm}} \times r_{i,t}\hat{d}_i}_{0} =$$

$$\hat{d}_i \cdot {}^I\vec{v}^{B_{cm}} + \hat{d}_i \cdot \left({}^I\vec{\omega}^B \times \vec{r}^{\,^{S_i/B_{cm}}}\right) \quad (10)$$

.

Note that this equation differs from the one presented by Kimball [1] in that each $\vec{r}^{\,^{S_i/B_{cm}}}$ corresponds to exactly one DVL sounding, as opposed to an averaging of the four beams. This treatment of the data avoids the potential for biases induced by fitting planes to nonplanar surfaces, and is one of the three major innovations of this extension.

D. Optimization Reduction

Equation 10 can be used to estimate the iceberg's motion parameters and reconstruct the shape of the iceberg using the method of Kimball. However, as in Kimball's method, the $\vec{r}^{\,^{S_i/B_{cm}}}$ points yield an inner loop matrix on the order of thousands of entries for the optimizer to invert at each iteration of the outer loop heading spline parameter search. Indeed, rather than there being three new equations per DVL ping, there are now four; it would appear at first that removing a source of potential bias has cost us an even larger optimization! However, by recognizing that the unknown vector $\vec{r}^{\,^{S_i/B_{cm}}}$, i.e. the "map feature locations" can be represented as the difference of other vectors that are either measured or are already being estimated, the iceberg-fixed points can be removed entirely from the optimization without loss of information. The inner loop parameters x_{ls} now consist only of the iceberg translation parameters $\vec{P}_x$ and not the map features.

Since the inner loop of the optimization grows roughly by the square of the number of such points, this can yield drastic speed increases in the overall solution. By Equation 6, the quantity in parentheses in 10 can be rewritten as

$$^I\vec{\omega}^B \times \vec{r}^{\,^{S_i/B_{cm}}} = {}^I\vec{\omega}^B \times \left(\vec{r}^{\,^{Vcm/O}} + \vec{r}^{\,^{S_i/V_{cm}}} - \vec{r}^{\,^{Bcm/O}}\right) \quad (11)$$

Substituting 11 into 10 and distributing the dot product yields the new equation

$$\hat{d}_i \cdot \underbrace{^I\vec{v}^{V_{cm}}}_{\text{known}} - \hat{d}_i \cdot \Big(\underbrace{^I\vec{\omega}^B}_{\text{outer loop}} \times \underbrace{\vec{r}^{\,^{Vcm/O}}}_{\text{known}} \Big) + \underbrace{\frac{dr_i}{dt}}_{\text{from DVL}}$$

$$= \hat{d}_i \cdot \left({}^I\vec{v}^{B_{cm}} - {}^I\vec{\omega}^B \times \vec{r}^{\,^{Bcm/O}} \right). \quad (12)$$

The terms of Equation 12 are arranged such that all terms that are either assumed known, measured, or estimated in the outer loop are on the left hand side, and all the terms estimated in the inner loop are on the right hand side. And now to do a strict accounting of the problem, noting the basis in which each vector is written, and writing out all necessary rotation matrices,

$$\underbrace{\hat{d}_i^\intercal \; {}^V R^I \left({}^I\vec{v}^{V_{cm}} - [{}^I\vec{\omega}^B]_\times \vec{r}^{\,^{Vcm/O}} \right) + \frac{dr_i}{dt}}_{\text{“Measurement” } i \text{ at time } j}$$

$$= \underbrace{\hat{d}_i^\intercal \; {}^V R^I \left((\dot{B}_x(t_j) - [{}^I\vec{\omega}^B]_\times B_x(t_j)) \right)}_{\text{one row of the measurement matrix}} \vec{P}_x. \quad (13)$$

where $[\quad]_\times$ is the matrix representation of the vector cross product, $B_x(t_j)$ is the $2 \times 2N_{\text{control points}}$ matrix of position spline basis functions evaluated at time t_j, and $\dot{B}_x(t_j)$ is the equivalent matrix for the basis derivatives. $\vec{P}_x$ are the iceberg position spline control points being estimated in the inner optimization loop.

The measurements and measurement matrix row for each time step are stacked to form an equation of the form $b = Ax$, where x is a vector of spline control points $\vec{P}_x$. With the iceberg-fixed sounding locations removed from the optimization, $x \in \mathbb{R}^{O(10)}$ where in previous methods, $x \in \mathbb{R}^{O(1000)}$. This speeds up the pseudoinverse calculation greatly.

E. Removal of Inertial Position from Optimization

The last contribution of this paper is the most important from a practical implementation standpoint. While the first two eliminate a small source of potential error and speed up the post-processing, the last contribution allows for the AUV to collect all data in a mapping run without the need for its host ship to provide it with navigation updates, potentially freeing the ship to perform other research tasks.

All work up to this point assumed that the inertial position and velocity of the vehicle are known. Indeed, for some tasks, it may be of interest to know how the iceberg moved while it was being mapped. However, if estimating the shape is the only goal of the mission (which is often the case in

mapmaking), the task can be completed entirely in relative terms.

This can be done by recasting the optimization using only iceberg-relative terms. Eliminating all the inertial terms in Equation 6 leaves the new loop equation

$$\vec{r}^{\,V_{cm}/B_{cm}} + \vec{r}^{\,S_i/V_{cm}} = \vec{r}^{\,S_i/B_{cm}} \tag{14}$$

Taking derivatives now in the iceberg frame,

$$\frac{^B d}{dt}\left(\vec{r}^{\,V_{cm}/B_{cm}} + \vec{r}^{\,S_i/V_{cm}} = \vec{r}^{\,S_i/B_{cm}}\right) \tag{15}$$

results in the new optimization equation

$$\hat{d}^{S_i/V_{cm}} \cdot {}^B\vec{v}^V + \frac{dr_i}{dt} + \underbrace{\hat{d}^{S_i/V_{cm}} \cdot \left({}^B\vec{\omega}^V \times \vec{r}^{\,S_i/V_{cm}}\right)}_{0} = 0 \tag{16}$$

$$\hat{d}_V^{S_i/V_{cm}} \cdot {}^B\vec{v}^{V_{cm}} = -\frac{dr_i}{dt} \tag{17}$$

This results in the normal DVL equation, but developed in the iceberg frame, rather than the inertial frame. Note that the unit vector $\hat{d}$ is expressed in the vehicle frame, because that is the frame in which it is fixed. In fact, without additional attitude and heading information, the DVL can only measure the vehicle's velocity *as expressed in the vehicle's own frame*. Thus, the need to know the vehicle's inertial position or to estimate the iceberg's velocity explicitly has been eliminated. However, the heading of the iceberg over the duration of the mapping run must still be estimated in order to resolve the DVL measurements into the iceberg frame.

$$\underbrace{\hat{d}_i^{\mathsf{T}}\,{}^V R^B}_{A}\ \underbrace{({}^B\vec{v}_B^{V_{cm}})}_{x} = \underbrace{-\frac{dr_i}{dt}}_{b} \tag{18}$$

The heading estimation of the iceberg is performed in the same manner as in [1], but the rest of the optimization (the entire inner loop) is essentially reduced to a check to see how well the loop closure constraint is satisfied.

IV. Results

The modified map estimation algorithm was implemented on a simulated moving iceberg, as well as on field data collected in Monterey Canyon to which simulated motion was added.

A. Simulation Results

The simulated vehicle followed a nominally circular path around a drifting iceberg. Gaussian noise was added to the multibeam and DVL soundings, as well as to the odometry. Figure 5(a) shows the resulting point cloud map of the iceberg using all available information, while 5(b) shows results from using a constant-motion model for the iceberg translation and rotation. Errors in motion modeling manifest themselves as warping in the map and misalignment between DVL and multibeam soundings. This is most evident in the top left corner of figure 5(b). Figure 6 shows the estimated iceberg rotation over the mapping run. The constant-slope (red line) was obtained by matching overlapping swaths at the end of the run, without using intermediate DVL measurements. The more accurate model (blue line) incorporated the DVL measurements in the manner described above.

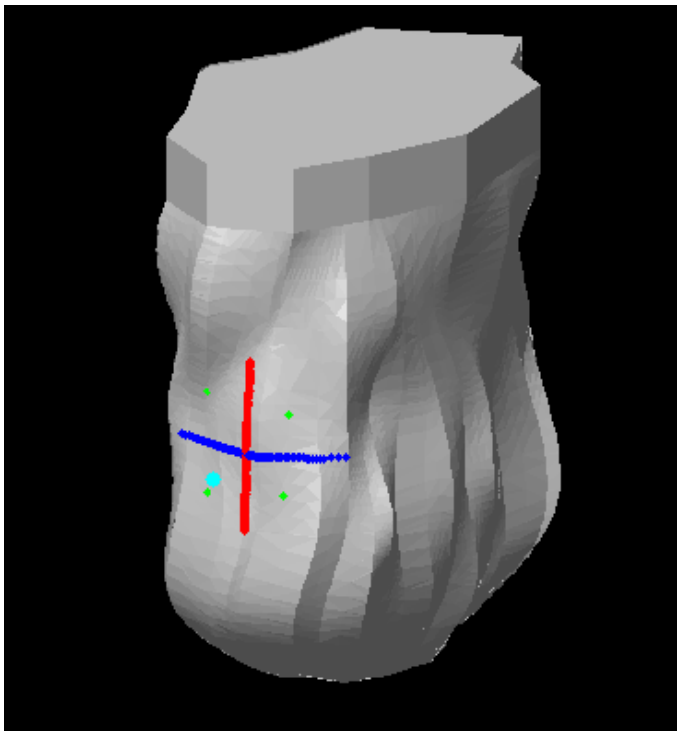

Fig. 4. Simulated iceberg and vehicle with ensonified points shown.

B. Field Data results

Data have been collected from underwater cliffs in Monterey Bay as a surrogate for Antarctic icebergs. Two passes by the canyon wall can be seen in Figure 7(a). A small, constant angular velocity was added to the motion of the vehicle to simulate the effects of iceberg motion, yielding the map shown in Figure 7(b). The estimation was carried out in purely relative terms as described in Section III-E. The results of the estimation can be seen in Figure 8. The blue ground track is the initial estimate based on the added motion, the green is the best estimate of "truth," based on dead reckoning using high-grade inertial sensors, and the red is the output of the estimation framework described in this paper. Overall, the algorithm does a good job in recovering from the added motion, and enforces loop closure with an RMS alignment error on the order of 1 meter. However, there remain slight discrepancies in the dead reckoned trajectory and the estimated solution, likely due to unmodeled sources of error like DVL bias and DVL dropout. Care needs to be taken in interpreting these discrepancies, as even the "truth data" contains such errors, and itself represents a best estimate of the trajectory, given different assumptions about the environment. The key point is that the algorithm was

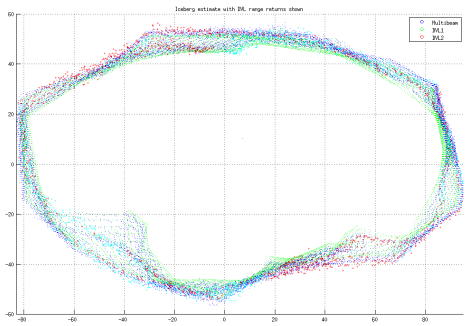

(a) Iceberg reconstruction using DVL measurements

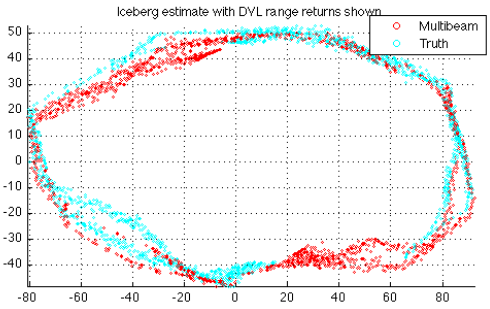

(b) Iceberg reconstruction without DVL measurements

Fig. 5. Top-view of reconstructions with and without DVL information

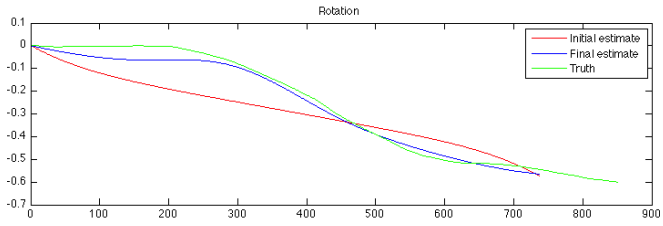

Fig. 6. Estimated and actual [simulated] iceberg motion

able to recover from the simulated motion of the canyon and create a self-consistent map to within the uncertainty of the map obtained by assuming a stationary world.

ACKNOWLEDGMENT

This work was funded by NASA ASTEP Grant NNX11AR62G.

The authors would like to thank the Monterey Bay Aquarium Research Institute for their support and Peter Kimball for laying a strong foundation.

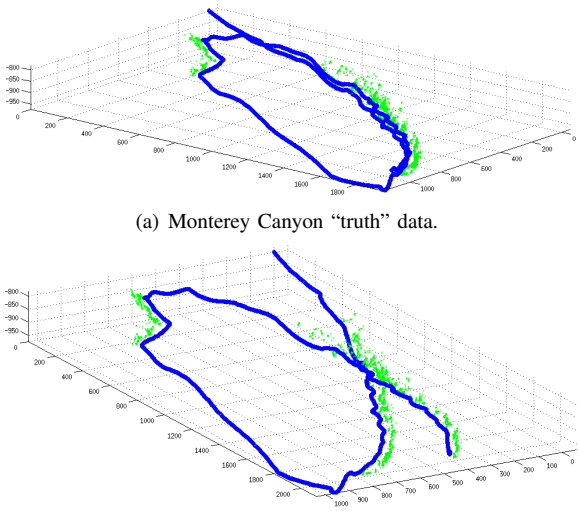

(a) Monterey Canyon "truth" data.

(b) Data corrupted with heading bias

Fig. 7. Top-view of reconstructions with and without DVL information. Blue points represent the trajectory. Green points are sonar sounding locations.

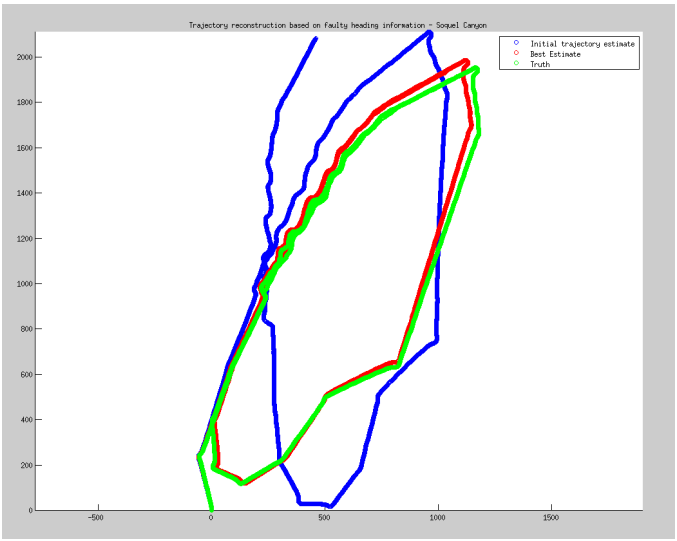

Fig. 8. Top-view of estimated vehicle trajectory through Monterey Canyon. Blue: initial estimate. Red: Mapping algorithm estimate. Green: "Truth"

REFERENCES

[1] P. Kimball and S. M. Rock, "Estimation of iceberg motion for mapping by auvs," in *IEEE-OES Autonomous Underwater Vehicles Conference (AUV)*, (Monterey, CA), 08/2010 2010.

[2] K. L. Smith, B. H. Robison, J. J. Helly, R. S. Kaufmann, H. A. Ruhl, T. J. Shaw, B. S. Twining, and M. Vernet, "Free-drifting icebergs: hot spots of chemical and biological enrichment in the weddell sea," *Science*, vol. 317, no. 5837, pp. 478–482, 2007.

[3] B. W. Hobson, A. D. Sherman, and P. R. McGill, "Imaging and sampling beneath free-drifting icebergs with a remotely operated vehicle," *Deep Sea Research Part II: Topical Studies in Oceanography*, vol. 58, no. 11, pp. 1311–1317, 2011.

[4] J. Bellingham, C. Goudey, T. Consi, J. Bales, D. Atwood, J. Leonard, and C. Chryssostomidis, "A second generation survey auv," in *Autonomous Underwater Vehicle Technology, 1994. AUV'94., Proceedings of the 1994 Symposium on*, pp. 148–155, IEEE, 1994.

[5] R. McEwen, H. Thomas, D. Weber, and F. Psota, "Performance of an auv navigation system at arctic latitudes," *Oceanic Engineering, IEEE Journal of*, vol. 30, no. 2, pp. 443–454, 2005.

[6] K. Nicholls, E. Abrahamsen, J. Buck, P. Dodd, C. Goldblatt, G. Griffiths, K. Heywood, N. Hughes, A. Kaletzky, G. Lane-Serff, *et al.*, "Measurements beneath an antarctic ice shelf using an autonomous underwater vehicle," *Geophysical Research Letters*, vol. 33, no. 8, 2006.

[7] N. S. Tervalon and R. Henthorn, "Ice profiling sonar for an auv: experience in the arctic," in *OCEANS'02 MTS/IEEE*, vol. 1, pp. 305–310, IEEE, 2002.

[8] P. Wadhams, M. Kristensen, and O. Orheim, "The response of antarctic icebergs to ocean waves," *Journal of Geophysical Research: Oceans (1978–2012)*, vol. 88, no. C10, pp. 6053–6065, 1983.

[9] S. Augenstein, *Monocular Pose and Shape Estimation of Moving Targets, for Autonomous Rendezvous and Docking*. Phd, Stanford University, 06/2011 2011.

[10] R. A. Newcombe, A. J. Davison, S. Izadi, P. Kohli, O. Hilliges, J. Shotton, D. Molyneaux, S. Hodges, D. Kim, and A. Fitzgibbon, "Kinectfusion: Real-time dense surface mapping and tracking," in *Mixed and augmented reality (ISMAR), 2011 10th IEEE international symposium on*, pp. 127–136, IEEE, 2011.

[11] P. J. Besl and N. D. McKay, "Method for registration of 3-d shapes," in *Robotics-DL tentative*, pp. 586–606, International Society for Optics and Photonics, 1992.

[12] P. Kimball, *Iceberg-Relative Navigation for Autonomous Underwater Vehicles*. Phd, Stanford University, Stanford, CA, 08/2011 2011.

[13] L. Piegl and W. Tiller, *The NURBS Book*. Springer Berlin, 1997.